

RESEARCH

Open Access



Unveiled stress dynamics: the role of post length and repair materials in perforated tooth models: a finite element analysis study

Nihan Çelik Uzun^{1*}, Altuğ Uşun² and Davut Çelik¹

Abstract

Background Post placement is a common practice to reinforce weakened roots. However, the choice of post length and repair material for root perforation influences the stress distribution within the dentin and surrounding tissues. This study aimed to evaluate the effects of post length and repair materials on the stress distribution in perforated tooth models through finite element analysis (FEA).

Methods A three-dimensional FEA model of a mandibular first molar tooth was created via Materialise 3-Matic software. Posts with lengths of 4 mm, 6 mm, and 8 mm inside the root and perforation areas in the middle third of the distal root were created. The control groups (CGs) included nonperforated models (CG4: Control group treated with 4 mm post, CG6: Control group treated with 6 mm post, CG8: Control group treated with 8 mm post) and those with unrepaired (UR) perforations (P) (P4/UR, P6/UR, P8/UR). MTA or Biodentine were used as repair materials for the main analysis groups (P4/MTA, P6/MTA, P8/MTA, P4/Biodentine, P6/Biodentine, P8/Biodentine); subsequently, all the models were restored with a ceramic crown. A 100 N force was applied through opposing teeth, and the maximum von Mises stress values and stress distributions in the model were analyzed.

Results The maximum von Mises stress values in P4/MTA, P6/MTA, P8/MTA, P4/Biodentine, P6/Biodentine, P8/Biodentine models were slightly lower than those in P4/UR, P6/UR, P8/UR models. In the perforated models, extending the post from 6 mm to 8 mm reduced the stresses in the dentin and the post, while increasing the stresses in the perforation area. P8/UR model had the highest stress value at 63.22 MPa, followed by P8/MTA (62.80 MPa) and P8/Biodentine (36.20 MPa), and the lowest stress value was in P6/Biodentine (15.92 MPa) in the perforation area. The lowest stress accumulation was observed in P8/Biodentine (0.036 MPa) model in the PDL.

Conclusions In perforated models, although the overall stresses in the dentine reduced with longer posts, the stresses in the perforation area increased. Biodentine enhances the mechanical stability of tooth structures and reduces stress concentrations, making it a suitable material for managing perforated teeth in post-endodontic restorations.

Keywords Root perforation, Finite element analysis, Dental fiber post, Biodentine, Mineral trioxide aggregate

*Correspondence:

Nihan Çelik Uzun
nihancelik@ktu.edu.tr

¹Faculty of Dentistry, Department of Endodontics, Karadeniz Technical University, Trabzon, Turkey

²Central Research Laboratory Application and Research Center, Department of Mechanical Engineering, Karadeniz Technical University, Trabzon, Turkey



© The Author(s) 2025. **Open Access** This article is licensed under a Creative Commons Attribution-NonCommercial-NoDerivatives 4.0 International License, which permits any non-commercial use, sharing, distribution and reproduction in any medium or format, as long as you give appropriate credit to the original author(s) and the source, provide a link to the Creative Commons licence, and indicate if you modified the licensed material. You do not have permission under this licence to share adapted material derived from this article or parts of it. The images or other third party material in this article are included in the article's Creative Commons licence, unless indicated otherwise in a credit line to the material. If material is not included in the article's Creative Commons licence and your intended use is not permitted by statutory regulation or exceeds the permitted use, you will need to obtain permission directly from the copyright holder. To view a copy of this licence, visit <http://creativecommons.org/licenses/by-nc-nd/4.0/>.

Background

Endodontically treated teeth exhibit reduced dentine resistance due to material loss, making them more prone to fractures [1]. Post-core restorations help preserve tooth structure and improve crown retention in compromised teeth [2, 3]. The resistance of a tooth to fracture is related to the stress distribution at the dentin/post interface [4]. In areas where stress accumulation is intense, the risk of bond failure and fracture between interfaces increases [5, 6].

The stress distribution on the root varies depending on the materials used for the posts and cores [7]. Metallic posts, which have a higher elastic modulus than dentine does, transmit more stress, increasing the risk of cracks and fractures [6, 8]. In contrast, fiber posts, with their lower elasticity, promote a more even distribution of chewing forces, thereby reducing stress on the root and minimizing the risk of fractures [8, 9]. Therefore, fiber posts are generally preferred for endodontically treated teeth with coronal damage, as they increase the stress distribution and lower the chances of fracture [10].

The stress distribution of fiber posts can be influenced by several factors, including the length, diameter, and design of the post [10]. It is therefore recommended that the post length should be at least two-thirds of the root length or clinical crown length. If these conditions cannot be met, the post length should extend to at least half of the root [11]. Numerous studies [5, 12–20] have examined the effects of the post length on the stress distribution and fracture resistance. Some research [12–15] indicates that longer posts lower stress in dentine and improve fracture resistance, whereas others show no difference in stress distribution between short and long posts [5, 16–20]. Additionally, studies indicate that longer posts may enhance retention by occupying more root space but can lead to greater dentine loss, potentially decreasing fracture resistance. In contrast, shorter posts offer lower retention [8, 14, 21]. Thus, the optimal post length for fiber posts remains undetermined.

On the other hand, selecting an inappropriate post size, misdirecting the post drill, or insufficient visibility during post preparation can lead to root perforation [22], which weakens the root and reduces the resistance of the tooth to fracture [23, 24]. Therefore, the selection of appropriate restoration techniques and biocompatible materials is critical. A variety of materials have been used for perforation repairs, but MTA is favored for its excellent sealing ability, biocompatibility, ability to support hard tissue formation, and antibacterial properties [25]. However, its drawbacks have spurred research into alternatives such as Biodentine, which aims to overcome the limitations of MTA [26]. While these materials improve tooth durability, understanding the biomechanical response of the tooth is important, as stress in the root can cause

cracks or exacerbate existing damage [27]. Determining actual clinical conditions in vivo or in the laboratory presents challenges [23]. Finite element analysis (FEA) generates standardized 3D models that simulate oral conditions throughout surgical phases, facilitating visualization of stress distribution [28]. Despite advancements in materials and techniques, data on the combined effects of post length and repair materials on the stress distribution, particularly in perforated teeth, are limited. Hence, this study aimed to evaluate the impact of varying post lengths and repair materials on the stress distribution in tooth models with perforations through FEA.

Methods

Preparation of the models

The tooth model was obtained from CT scans and adjusted via Wheeler's dental atlas [29]. On the basis of the geometry of a real tooth, a 3D model of a mandibular first molar and surrounding structures was created with Materialise 3-Matic software. The crown height was 6.7 mm, with the roots measuring 12 mm. The bone structure was modeled 2 mm below the crown, including a 0.2 mm thick periodontal ligament (PDL) and both cortical and cancellous bones [30].

Posts of 4 mm, 6 mm, and 8 mm length (1/3, 1/2, and 2/3 of the root length, respectively) were designed with a 0.8 mm apical diameter and an 8% taper [31]. The remaining canal was filled with gutta-percha on the basis of post length. The perforation models included a perforation with both the entrance and exit diameters measuring 2 mm in the middle third of the distal root, extending to the PDL (Supplementary material 1a) [23]. A 2 mm dentine layer simulated the ferrule effect, whereas a 4 mm composite resin core had 6° inclined walls [32, 33]. A ceramic crown was fitted with a 1 mm side step around the dentin (Supplementary material 1b).

A total of 12 models were created to analyze the effects of post length and perforation repair. The control groups (CG) included nonperforated models (CG4: Control group treated with 4 mm post, CG6: Control group treated with 6 mm post, CG8: Control group treated with 8 mm post) and those with unrepaired (UR) perforations (P) (P4/UR, P6/UR, P8/UR). The main analysis groups featured perforations repaired with MTA or Biodentine (P4/MTA, P6/MTA, P8/MTA, P4/Biodentine, P6/Biodentine, P8/Biodentine) (Table 1). The medium-length post (6 mm) was positioned at the midpoint of the perforation, whereas the shorter post (4 mm) ended just before the perforation area. The longer post (8 mm) extended beyond the perforation to evaluate the impact of additional support (Fig. 1a).

Table 1 Overview of the experimental models

	Model name	Perforation	Perforation repair material	Post length (mm)	
Control groups	CG4	X	X	4	
	CG6	X	X	6	
	CG8	X	X	8	
	P4/UR	✓	X	4	
	P6/UR	✓	X	6	
	P8/UR	✓	X	8	
	Main analysis groups	P4/MTA	✓	MTA	4
		P6/MTA	✓	MTA	6
P8/MTA		✓	MTA	8	
P4/Biodentine		✓	Biodentine	4	
P6/Biodentine		✓	Biodentine	6	
P8/Biodentine		✓	Biodentine	8	

CG: Control group, P:Perforation, UR: Unrepaired, MTA and Biodentine specify the perforation repair material used in the model names

Preparation of the finite element models

The models were exported as “stl” files from Materialise 3-Matic and improved in Meshmixer. They were then imported into Hypermesh, where surface modeling uses triangular elements, followed by remeshing with 3D elements for a uniform and accurate mesh.

Mesh and timeline convergence analysis

Convergence analysis was performed on the 6 mm post and MTA models to ensure that the results were not affected by mesh quality or timestep parameters. The simulations were run with finer meshes and smaller timesteps to create a convergence curve.

Finite element analysis

After the model was prepared, the 3D meshes were exported to LS-DYNA for FEA. Most materials were modeled as linear elastic, homogeneous, and isotropic, except for the fiberglass post, which was treated as orthotropic. Perfect contact between materials was assumed with surface-to-surface contact and no contact failure, as the expected stresses remain below the yield strength. The linear implicit solving method was used because of the absence of dynamic forces. Table 2 provides the elastic modulus and Poisson’s ratio for the materials, including the modeled dental supporting tissues [30, 34]. A 0.2 mm resin cement layer was added at the interface between the core and crown and between the post and dentine.

Loading conditions

The model was fixed at the base with cancellous bone for loading. A soft material was incorporated to simulate the chewing motion, enhancing the accuracy of the force distribution on the crown, as influenced by the maxillary tooth (Supplementary material 2). A force of 100 N was

applied through opposing teeth to achieve a more realistic representation of mastication [3, 35] (Fig. 1b). The maximum values of von Mises stress in the dentin (overall tooth), post, perforation area, cortical bone, and PDL were subsequently analyzed.

Results

Results of the convergence analyses

Convergence analyses were conducted to determine the appropriate mesh size and timestep values. The mesh density was gradually increased, as shown in Fig. 2a, and analyses were carried out accordingly. The maximum von Mises stress values on the model were measured, and the results are plotted in Fig. 2b, which shows the stress values relative to the number of elements. The results indicated that exceeding 700,000 elements did not alter the outcomes, confirming that this count was sufficient for accuracy, corresponding to an element size of 0.08 mm in the perforation area and up to 1 mm in low-stress regions. Similarly, more than 1,000 steps were needed for stable implicit testing results (Fig. 2c).

Maximum stresses and distributions in the models

The analysis involved multiple models, focusing on different post lengths (4 mm, 6 mm, and 8 mm) and the effects of various repair materials, allowing for a thorough comparison of their mechanical properties. As indicated in Table 3, the lowest von Mises stress values observed in the dentin (overall tooth) were recorded for the control groups, including the nonperforated models (CG4: 7.04, CG6: 6.84, CG8: 6.23). The maximum von Mises stress values in the models repaired with MTA (P4/MTA, P6/MTA, P8/MTA) or Biodentine (P4/Biodentine, P6/Biodentine, P8/Biodentine) were slightly lower than those in the unrepaired perforated models (P4/UR, P6/UR, P8/UR) (Table 3). Figure 3 shows the stress distributions in dentin (overall tooth), where the CG models exhibit uniform stress. Increasing the post length notably reduces the stress, with the 8 mm post length showing the most uniform distribution.

Table 3 shows that the maximum von Mises stress values for the posts were generally greater in the perforated models (P4/UR, P6/UR, P8/UR, P4/MTA, P6/MTA, P8/MTA, P4/Biodentine, P6/Biodentine, P8/Biodentine) compared to CGs (CG4, CG6, CG8), decreasing with longer posts. The 8 mm posts had the lowest values (99.03 for CG8, 113.30 for P8/UR, 113.00 for P8/MTA, and 113.30 for P8/Biodentine). Repairing perforations with MTA or Biodentine did not affect the stress values of the posts. For 8 mm posts, stress was evenly spread between the top and perforation, indicating an effective force distribution. In contrast, the 6 mm posts presented greater stress in the middle, whereas the 4 mm posts presented concentrated stress at the top (Fig. 3).

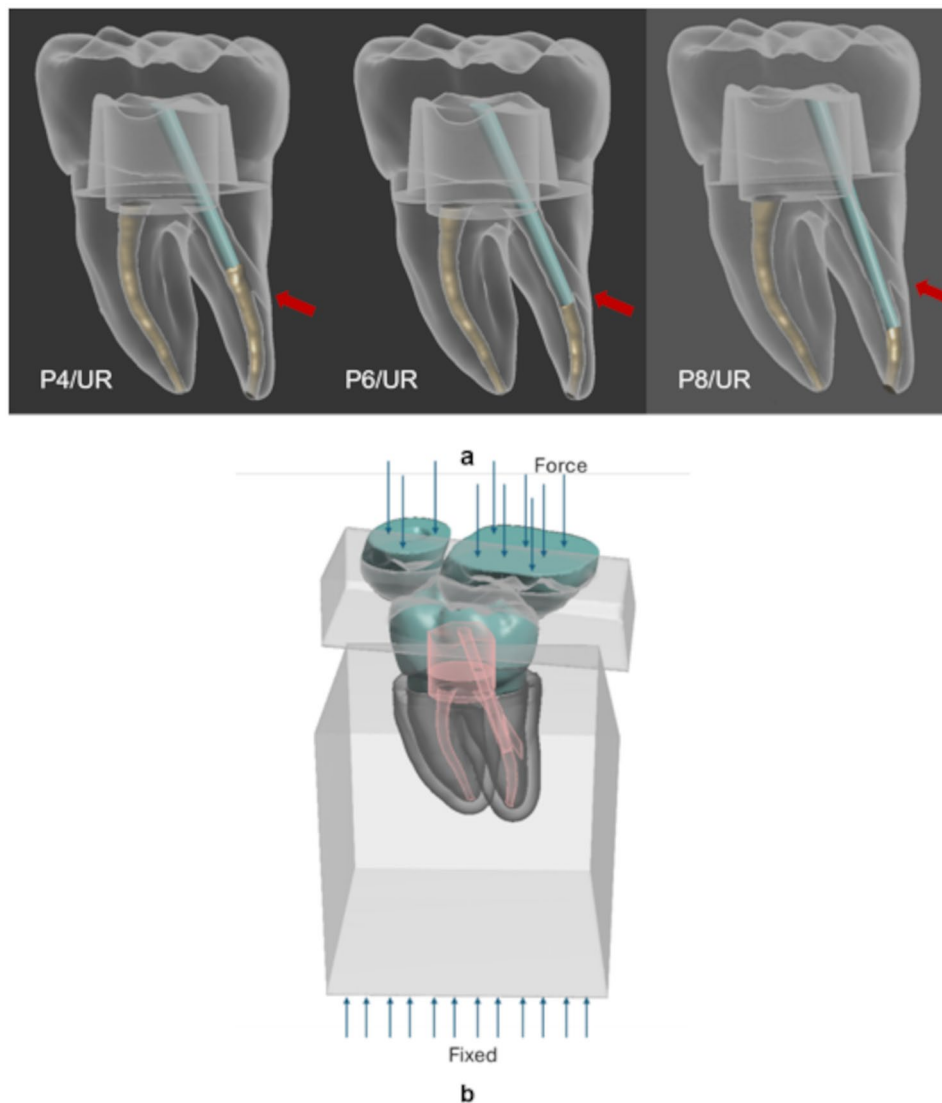


Fig. 1 (a) Unrepaired perforation models with different post lengths; P4/UR: unrepaired model with a 4 mm post, P6/UR: unrepaired model with a 6 mm post, P8/UR: unrepaired model with a 4 mm post, red arrow: perforation area (b) Model under loading conditions

In the CG models, the maximum von Mises stress values in the perforation areas (CG4: 4.41, CG6: 4.21, CG8: 5.61) were lower than those in the perforated models. Among the perforated models, the P8/UR model had the highest stress value at 63.22 MPa, followed by P8/MTA (62.80 MPa) and P8/Biodentine (36.20 MPa), and the lowest stress value was in P6/Biodentine (15.92 MPa) (Table 3). Figure 3 shows the stress distribution in the perforation area, revealing more homogeneous stress in the CG models. In the perforated models, the maximum stress was concentrated around the perforation area. As shown, for post lengths of 4 mm and 6 mm, the load is transferred primarily to the upper section of the root where the repair material is applied. In contrast, when the post length is increased to 8 mm, the primary stress

shifts to the lower regions of the canal, where the longer post length transfers the load.

The stress values on the cortical bone did not change with variations in repair materials or post length. In the perforated models, slightly lower maximum von Mises stress values were observed in the PDL than in the CG models. The lowest stress accumulation was observed in P8/Biodentine (0.036 MPa) (Table 3).

Discussion

Damage in areas of high stress can compromise the strength of dentin. With the increasing use of fiber and resin-reinforced posts, determining the appropriate depth of insertion has become crucial for clinicians [5]. Furthermore, although few studies exist, perforations in the root affect the stress distribution in dentin [23, 36,

Table 2 Materials used in the finite element analysis and their mechanical properties

Material	Elasticity Modulus (MPa)	Poisson's Ratio
Dentin	18,600	0.31
Cortical Bone	13,700	0.3
Cancellous Bone	1370	0.3
Ceramic crown	65,000	0.19
Composite Resin	16,400	0.28
Gutta-Percha	140	0.45
Resin cement	8300	0.35
MTA	11,760	0.314
Biodentine	22,000	0.33
Periodontal ligament	0.0689	0.45
Post		
x	37,000	0.34
y	9500	0.27
z	9500	0.27

[37]. To our knowledge, this study is the first to use FEA to evaluate how different post lengths and repair materials influence the stress distribution following perforation and repair. Furthermore, this study aimed to fill this gap, providing valuable insights for optimizing treatment outcomes.

The stress distribution can be visualized through FEA, which simulates real oral conditions, and the perforation areas can be examined [28]. To ensure reliable results from FEA, the model must accurately reflect real conditions [38]. Chewing forces create stress on teeth, which is influenced by the load angle and geometry [39, 40]. While many studies [23, 41–43] apply force from one direction, a more realistic method simulates food particles between opposing teeth [21]. In our study, we incorporated opposing teeth to better mimic the natural force distribution instead of applying stress as a point load.

A 2 mm ferrule height is advised to ensure structural integrity in endodontically treated teeth [44], as stress levels change with it [12, 17, 45]. Our study utilized a mandibular molar tooth model with a 2 mm ferrule height to isolate the impact of ferrule height on stress distribution.

This study examined how varying post lengths affect structural integrity and stress distribution in models, especially around perforations. Yoon et al. [46] reported that distal post models in mandibular first molars presented stress values similar to those without posts, suggesting that the distal canal is best for post placement. Therefore, we simulated various post lengths in the distal canal of the molars.

According to our findings, the control groups included nonperforated models (CG4, CG6, CG8), which presented lower von Mises stress in the dentin (overall tooth) and perforation areas than did the perforated models (P4/UR, P6/UR, P8/UR, P4/MTA, P6/MTA, P8/

MTA, P4/Biodentine, P6/Biodentine, P8/Biodentine) across all post lengths. The stress concentration in the perforated models highlighted weaknesses in the dentin, confirming that perforation led to increased localized stress. This finding supports Askerbeyli et al. [37], who reported lower von Mises stress in root-filled models than in furcal perforated models. However, despite the repairs in our study, the stress values in dentin were still greater than those in CG models, which is consistent with Elwazen et al. [36], who noted greater stress in models repaired with MTA or Biodentine than in endodontically treated teeth, suggesting a loss of structural integrity in dentin.

In this study, the perforated models presented higher stress values on the post than did the CG models did, indicating that structural degradation caused by perforation increases the stress transferred to the remaining dentin and the post, as shown in Table 3. Additionally, the nonperforated models (CGs) exhibited an even stress distribution. In contrast, in the perforated models with short posts (P4/UR, P4/MTA, P4/Biodentine), stress tended to concentrate in the coronal region and progressively increased around the central perforation area with longer posts. Previous studies [4, 12, 39, 47] align with our findings, showing that longer posts distribute forces more evenly across both the cervical and apical areas, whereas shorter posts concentrate forces in the upper regions because of a higher center of rotation [48].

Our study revealed that increasing the post length reduces the stress values in both the post and the dentin, with the 8 mm post showing the best stress distribution. These findings align with previous studies [11, 12, 14], which reported that longer posts absorb more stress rather than transferring it to the dentin, resulting in a more homogeneous force distribution than shorter posts do. Ishak et al. [12] also noted that in a class 3 lever system, shorter posts accumulate more stress because of the need for greater forces near the fulcrum. However, when the stress values in the perforation area are analyzed, an interesting trend is that the stress values increase from 6 mm to 8 mm post length. When the post length is increased to 8 mm, the primary stress shifts to the lower regions of the canal. As the length of the root canal where the post is placed increases, the stress concentration that arises with the reduction in the dentin cross-section increases [49, 50]. Since the perforation area is a weak zone where stress accumulates, longer posts that make more contact with the area of the perforation carry more load to the perforation region. In contrast, shorter posts have less effect because they are located further away from the perforation area, which also explains why there is less stress accumulation in short posts in the current study. Additionally, this can be explained by the fact that

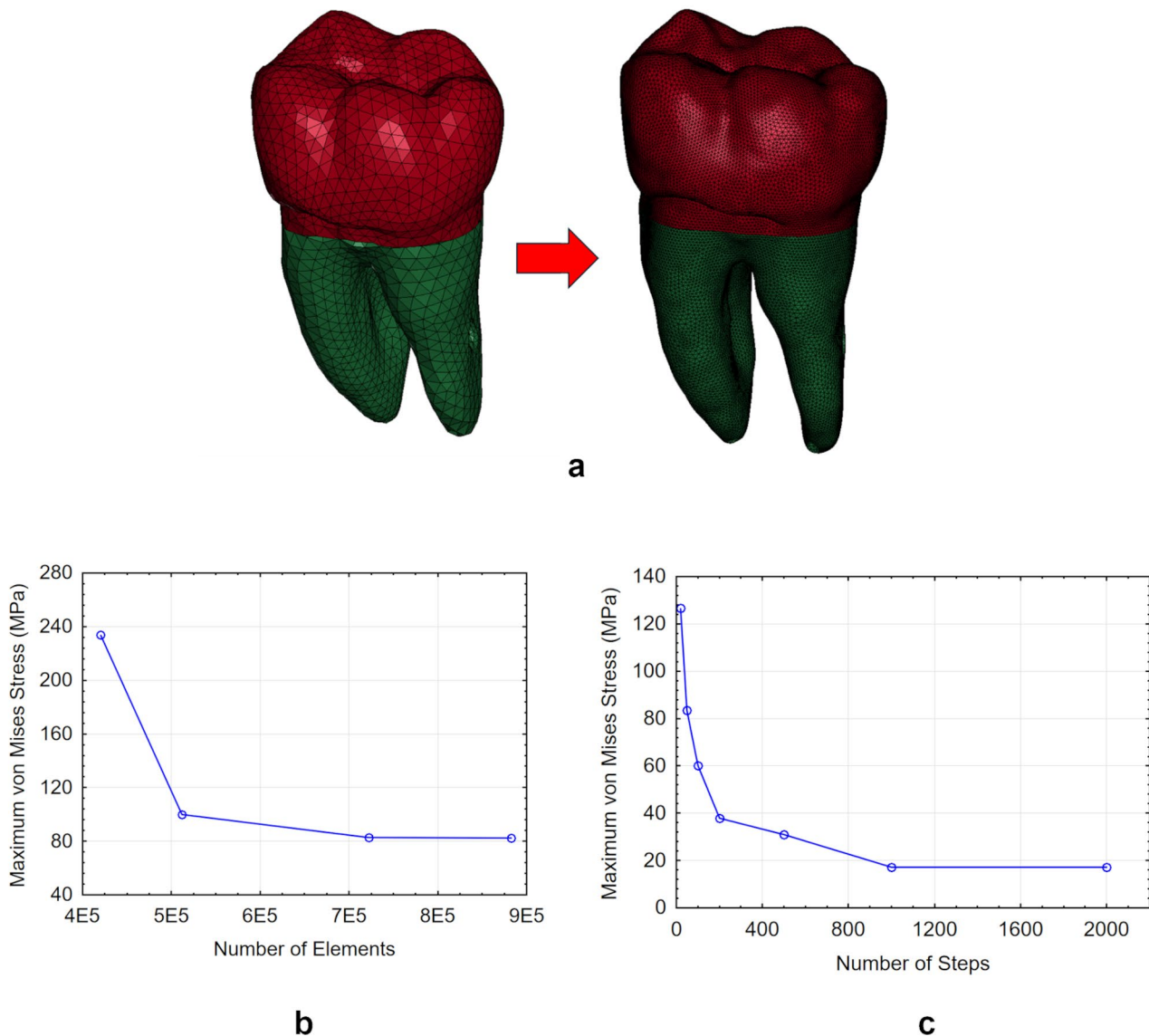


Fig. 2 Convergence analyses; (a) schematic of mesh size refinement; (b) number of elements that converge; (c) number of steps that converge

longer posts create a larger bending moment, thereby increasing the stress in the perforation area [51].

According to our findings, the stress values of the repaired models (P4/MTA, P6/MTA, P8/MTA, P4/Biodentine, P6/Biodentine, P8/Biodentine) showed lower stress values than unrepaired models (P4/UR, P6/UR, P8/UR), highlighting that the lack of supportive materials leads to higher stress concentrations in dentin, which weakens it [23, 34, 52]. Additionally, in our study, while material selection did not effectively affect the stress values in the overall tooth and post, it did lead to differences in the stress values in the perforation area. Compared with MTA, Biodentine resulted in lower stress values in the perforation area. Aslan et al. [23] reported that Biodentine’s lower von Mises stress results from its

superior elasticity. Materials with similar elastic modulus absorb stress differently; those closer to dentin (Biodentine) absorb more stress and transmit less stress to dentin. Therefore, as shown in Table 2, compared with that of MTA, the modulus of elasticity of Biodentine was closer to that of dentin, resulting in greater stress absorption and less stress transmission to the dentin in the perforation area.

The stress values on the cortical bone did not change with variations in repair materials or post length. Additionally, in the perforated models, slightly lower maximum stress values were observed in the PDL than in the CG models. As shown in Table 3, the stress generated in the perforated models may have concentrated in the perforation area and other regions, reducing the stress

Table 3 Maximum von Mises stress values in the models (the values are in MPa)

Model Name	Overall Tooth	Perforation Area	Post	Cortical Bone	PDL
CG4	7.04	4.41	176.80	7.40	0.047
CG6	6.84	4.21	137.38	6.53	0.084
CG8	6.23	5.61	99.03	8.26	0.059
P4/UR	16.01	28.21	173.33	7.37	0.046
P6/UR	17.85	22.13	173.30	7.35	0.045
P8/UR	14.90	63.22	113.30	6.70	0.050
P4/MTA	23.45	22.02	173.30	7.37	0.046
P6/MTA	17.51	20.34	177.10	7.35	0.045
P8/MTA	13.40	62.80	113.00	6.70	0.051
P4/Biodentine	16.0	18.04	173.70	7.37	0.048
P6/Biodentine	17.10	15.92	174.47	7.06	0.041
P8/Biodentine	13.20	36.20	113.30	6.78	0.036

CG: Control group, P: Perforation, UR: Unrepaired

experienced by the surrounding PDL. Furthermore, the lowest stress accumulation in the P8/Biodentine model can be explained by the mechanical support provided by the long post and the fact that Biodentine accumulates stress internally, preventing direct transmission of loads to the PDL.

The FEA used is a reliable method for simulating oral conditions; however, the results may vary owing to anatomical differences [28], which is one of the limitations of this study. Additionally, despite the anisotropic structure of dentin, it has been assumed that all the tissues are homogeneous, which may complicate the reflection of the results. It is important to support the accuracy of FEA with clinical trials. Additionally, factors such as the post material, design, and location of the perforation can also influence the stress distribution. Future studies should investigate these parameters and optimize them appropriately for clinical scenarios.

Conclusions

Under the limitations of this study:

- Longer (8 mm) posts decreased the maximum stress values in both the dentin and the post, enhancing the stress distribution by better transferring forces to surrounding areas. However, in cases with structural defects such as perforations, longer posts led to increased local stress in the perforation area.

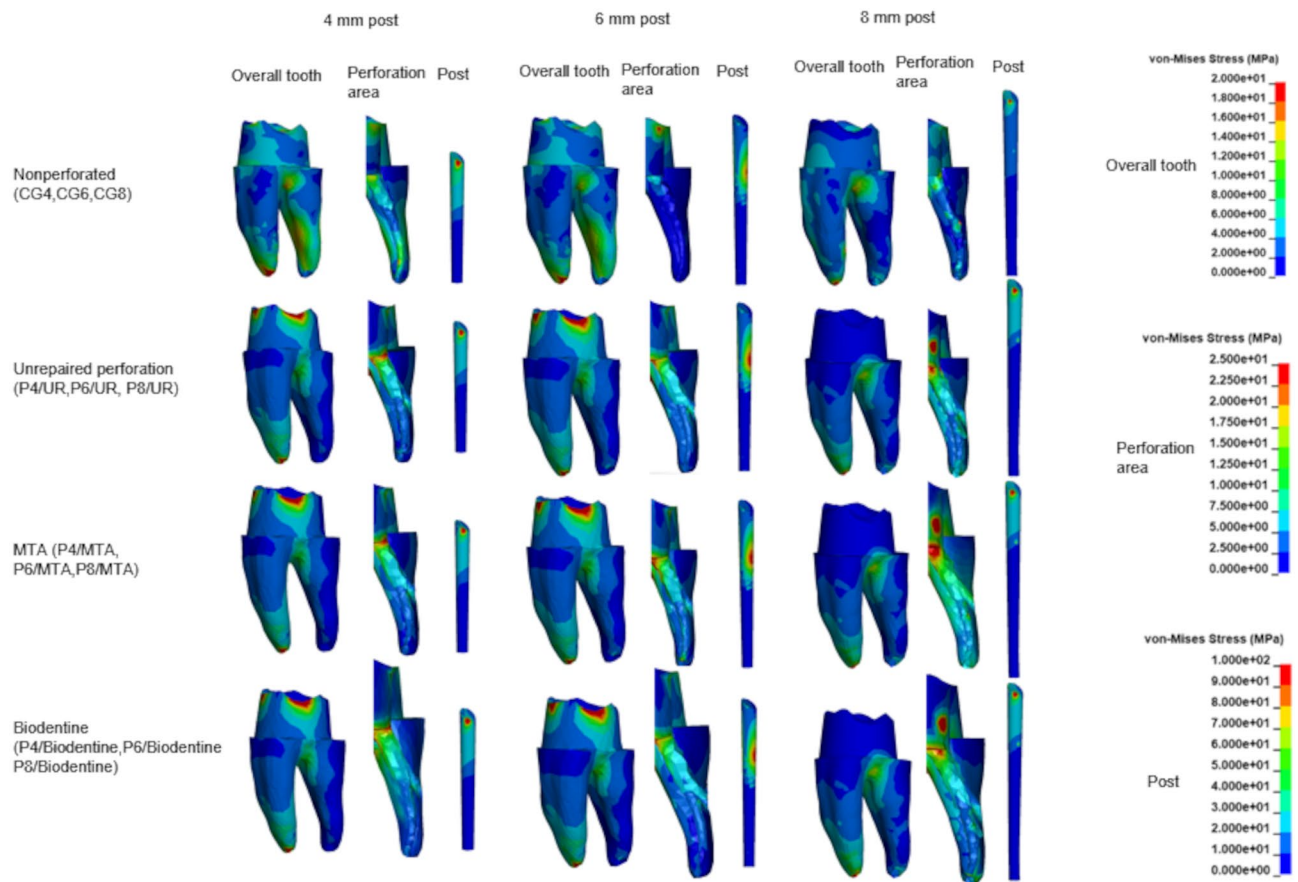


Fig. 3 Stress distributions in the overall tooth, perforation area, and post
CG: Control group, P: Perforation, UR: Unrepaired

- The repair of the perforation area reduces the stress in the dentin and perforation areas.
- While post length had a greater effect on the stress distribution than did the repair material, Biodentine had the best overall results for the perforation area.
- Although no significant difference in stress values was noted in the cortical bone, the higher stress values in the perforated models led to slightly reduced stress exposure for the PDL due to the distribution of stress between the perforation area and the surrounding structures.
- These results emphasize the importance of a balanced approach that considers both mechanical stability and localized stress effects when designing restorative strategies for perforated teeth.

Abbreviations

FEA	Finite element analysis
PDL	Periodontal ligament
UR	Unrepaired
CG	Control group
P	Perforation

Supplementary Information

The online version contains supplementary material available at <https://doi.org/10.1186/s12903-025-05750-8>.

Supplementary material 1: Schematic images of the mandibular molar tooth; (a) designed 6 mm post model with perforation area repaired with MTA, Biodentine or empty, (b) the bone structure, periodontal ligament, ferrule design, and crown

Supplementary Material 2: Simulation of the chewing motion with a soft material

Acknowledgements

This FEA study was conducted at Karadeniz Technical University, Medical Device Design and Production Application and Research Center, Trabzon.

Author contributions

All authors contributed to the study conception and design and authors' contributions were listed: Conceptualization: NÇU, DÇ, AU; Writing- Original draft preparation: NÇU, DÇ; Investigation: NÇU, AU, DÇ; Methodology: AU; Software: AU; Resources: AU; Supervision: DÇ; Writing-Reviewing and Editing: NÇU, DÇ.

Funding

This research did not receive any specific grant from funding agencies in the public, commercial, or not-for-profit sectors.

Data availability

The datasets used and/or analysed during the current study are available from the corresponding author on reasonable request.

Declarations

Ethics approval and consent to participate

Not applicable.

Consent for publication

Not applicable.

Competing interests

The authors declare no competing interests.

Received: 15 January 2025 / Accepted: 4 March 2025

Published online: 26 April 2025

References

1. da Silva PB, Duarte SF, Alcalde MP, Duarte MAH, Vivan RR, da Rosa RA, et al. Influence of cervical preflaring and root Canal Preparation on the fracture resistance of endodontically treated teeth. *BMC Oral Health*. 2020;20:111.
2. Nahar R, Mishra SK, Chowdhary R. Evaluation of stress distribution in an endodontically treated tooth restored with four different post systems and two different crowns- A finite element analysis. *J Oral Biol Craniofac Res*. 2020;10:719–26.
3. Li LL, Wang ZY, Bai ZC, Mao Y, Gao B, Xin HT, et al. Three-dimensional finite element analysis of weakened roots restored with different cements in combination with titanium alloy posts. *Chin Med J (Engl)*. 2006;119:305–11.
4. Memon S, Mehta S, Malik S, Nirmal N, Sharma D, Arora H. Three-dimensional finite element analysis of the stress distribution in the endodontically treated maxillary central incisor by glass fiber post and dentin post. *J Indian Prosthodont Soc*. 2016;16:70–4.
5. Chuang SF, Yaman P, Herrero A, Dennison JB, Chang CH. Influence of post material and length on endodontically treated incisors: an in vitro and finite element study. *J Prosthet Dent*. 2010;104:379–88.
6. Lertchirakarn V, Palamara JE, Messer HH. Patterns of vertical root fracture: factors affecting stress distribution in the root Canal. *J Endod*. 2003;29:523–8.
7. Badami V, Ketineni H, Pb S, Akarapu S, Mittapalli SP, Khan A. Comparative evaluation of different post materials on stress distribution in endodontically treated teeth using the finite element analysis method: A systematic review. *Cureus*. 2022;14:e29753.
8. Adanir N, Belli S. Evaluation of different post lengths' effect on fracture resistance of a glass fiber post system. *Eur J Dent*. 2008;2:23–8.
9. Theodosopoulou JN, Chochlidakis KM. A systematic review of dowel (post) and core materials and systems. *J Prosthodont*. 2009;18:464–72.
10. Tinaz AC, Alaçam T, Topuz O, Er O, Maden M. Lateral perforation in parallel post space preparations. *J Contemp Dent Pract*. 2004;5:42–50.
11. Giovani AR, Vansan LP, de Sousa Neto MD, Paulino SM. In vitro fracture resistance of glass-fiber and cast metal posts with different lengths. *J Prosthet Dent*. 2009;101:183–8.
12. Ishak MI, Ahmad Shafi A, Abdul Kadir MR, Sulaiman E. Effect of ferrule height and post length on mechanical stress and displacement of endodontically treated maxillary central incisor: a finite element analysis. *J Med Biol Eng*. 2017;37:336–44.
13. Lin J, Matinlinna JP, Shinya A, Botelho MG, Zheng Z. Effect of fiber post length and abutment height on fracture resistance of endodontically treated premolars prepared for zirconia crowns. *Odontology*. 2018;106:215–22.
14. Jindal S, Jindal R, Mahajan S, Dua R, Jain N, Sharma S. In vitro evaluation of the effect of post system and length on the fracture resistance of endodontically treated human anterior teeth. *Clin Oral Investig*. 2012;16:1627–33.
15. Amarnath GS, Swetha MU, Muddugangadhar BC, Sonika R, Garg A, Rao TR. Effect of post material and length on fracture resistance of endodontically treated premolars: an In-Vitro study. *J Int Oral Health*. 2015;7:22–8.
16. Hsu ML, Chen CS, Chen BJ, Huang HH, Chang CL. Effects of post materials and length on the stress distribution of endodontically treated maxillary central incisors: a 3D finite element analysis. *J Oral Rehabil*. 2009;36:821–30.
17. Santos-Filho PC, Veríssimo C, Soares PV, Saltarello RC, Soares CJ, Marcondes Martins LR. Influence of ferrule, post system, and length on Biomechanical behavior of endodontically treated anterior teeth. *J Endod*. 2014;40:119–23.
18. Franco EB, Lins do Valle A, Pompéia F, de Almeida AL, Rubo JH, Pereira JR. Fracture resistance of endodontically treated teeth restored with glass fiber posts of different lengths. *J Prosthet Dent*. 2014;111:30–4.
19. Santos-Filho PCF, Castro CG, Silva GR, Campos RE, Soares CJ. Effects of post system and length on the strain and fracture resistance of root filled bovine teeth. *Int Endod J*. 2008;41:493–501.
20. Schmitter M, Rammelsberg P, Lenz J, Scheuber S, Schweizerhof K, Rues S. Teeth restored using fiber-reinforced posts: in vitro fracture tests and finite element analysis. *Acta Biomater*. 2010;6:3747–54.
21. Boschian Pest L, Guidotti S, Pietrabissa R, Gagliani M. Stress distribution in a post-restored tooth using the three-dimensional finite element method. *J Oral Rehabil*. 2006;33:690–7.
22. Estrela C, Decurcio DA, Rossi-Fedele G, Silva JA, Guedes OA, Borges ÁH. Root perforations: a review of diagnosis, prognosis and materials. *Braz Oral Res*. 2018;32:e73.

23. Aslan T, Esim E, Üstün Y, Dönmez Özkan H. Evaluation of stress distributions in mandibular molar teeth with different iatrogenic root perforations repaired with Biodentine or mineral trioxide aggregate: A finite element analysis study. *J Endod.* 2021;47:631–40.
24. McCabe PS. Avoiding perforations in endodontics. *J Ir Dent Assoc.* 2006;52:139–48.
25. Juárez Broon N, Bramante CM, de Assis GF, Bortoluzzi EA, Bernardineli N, de Moraes IG, et al. Healing of root perforations treated with mineral trioxide aggregate (MTA) and Portland cement. *J Appl Oral Sci.* 2006;14:305–11.
26. Camilleri J. Investigation of Biodentine as dentine replacement material. *J Dent.* 2013;41:600–10.
27. Kishen A, Kumar GV, Chen NN. Stress-strain response in human dentine: rethinking fracture predilection in postcore restored teeth. *Dent Traumatol.* 2004;20:90–100.
28. Ainarsang A, Adarsha MS, Meena N, Vikram R, Gowda V, Harti SA. Effect of pulpal floor perforation repair on Biomechanical response of mandibular molar: A finite element analysis. *J Conserv Dent.* 2021;24:502–7.
29. Nelson SJ. Wheeler's dental anatomy, physiology and Occlusion-E-Book: Wheeler's dental anatomy, physiology and Occlusion-E-Book. 10th ed. Elsevier Health Sciences; 2014.
30. Helal MA, Wang Z. Biomechanical assessment of restored mandibular molar by endocrown in comparison to a glass Fiber Post-Retained conventional crown: 3D finite element analysis. *J Prosthodont.* 2019;28:988–96.
31. Hatta M, Shinya A, Vallittu PK, Shinya A, Lassila LV. High volume individual fibre post versus low volume fibre post: the fracture load of the restored tooth. *J Dent.* 2011;39:65–71.
32. Asmussen E, Peutzfeldt A, Sahafi A. Finite element analysis of stresses in endodontically treated, dowel-restored teeth. *J Prosthet Dent.* 2005;94:321–29.
33. Dejak B, Mlotkowski A, Romanowicz M. Finite element analysis of stresses in molars during clenching and mastication. *J Prosthet Dent.* 2003;90:591–97.
34. Belli S, Eraslan O, Eskitaşcıoğlu G. Effect of different treatment options on biomechanics of immature teeth: A finite element stress analysis study. *J Endod.* 2018;44:475–9.
35. Chieruzzi M, Pagano S, Cianetti S, Lombardo G, Kenny JM, Torre L. Effect of fibre posts, bone losses and fibre content on the Biomechanical behaviour of endodontically treated teeth: 3D-finite element analysis. *Mater Sci Eng C Mater Biol Appl.* 2017;74:334–46.
36. Elwazan GI, Roshdy NN, Abdelaziz S. Effect of mid-root perforation and its repair on stress distribution and fracture resistance: a 3D finite element analysis and in vitro study. *BMC Oral Health.* 2024;24:1340.
37. Askerbeyli Örs S, Aksel H, Küçükaya Eren S, Serper A. Effect of perforation size and furcal lesion on stress distribution in mandibular molars: a finite element analysis. *Int Endod J.* 2019;52:377–84.
38. Akbaş M, Akbulut MB, Belli S. Sonlu Elemanlar Stres analizi ve endodontide Kullanımı. *Eur J Res Dent.* 2021;5:99–108.
39. Agarwal SK, Mittal R, Singhal R, Sarah H, Kanchan C. Stress evaluation of maxillary central incisor restored with different post materials: a finite element analysis. *J Clin Adv Dent.* 2020;4:22–7.
40. Cailleateau JG, Rieger MR, Akin JE. A comparison of intracanal stresses in a post-restored tooth utilizing the finite element method. *J Endod.* 1992;18:540–4.
41. Er O, Kilic K, Esim E, Aslan T, Kilinc HI, Yildirim S. Stress distribution of oval and circular fiber posts in amandibular premolar: a three-dimensional finite element analysis. *J Adv Prosthodont.* 2013;5:434–9.
42. Çoban Öksüzer M, Şanal Çıkman A. Evaluation of fracture strength after repair of cervical external resorption cavities with different materials. *J Endod.* 2024;50:85–95.
43. González-Lluch C, Pérez-González A. Analysis of the effect of design parameters and their interactions on the strength of dental restorations with endodontic posts, using finite element models and statistical analysis. *Comput Methods Biomech Biomed Engin.* 2016;19:428–39.
44. Zhi-Yue L, Yu-Xing Z. Effects of post-core design and ferrule on fracture resistance of endodontically treated maxillary central incisors. *J Prosthet Dent.* 2003;89:368–73.
45. Mosharaf R, Abolhasani M, Fathi AH, Rajabi A. The effect of ferrule/crown ratio and post length on the applied stress and strain distribution to the endodontically treated maxillary central teeth: A finite element analysis. *Front Dent.* 2023;20:16.
46. Yoon HG, Oh HK, Lee DY, Shin JH. 3-D finite element analysis of the effects of post location and loading location on stress distribution in root canals of the mandibular 1st molar. *J Appl Oral Sci.* 2018;26:e20160406.
47. Pegoretti A, Fambri L, Zappini G, Bianchetti M. Finite element analysis of a glass fibre reinforced composite endodontic post. *Biomaterials.* 2002;23:2667–82.
48. Ko CC, Chu CS, Chung KH, Lee MC. Effects of posts on dentin stress distribution in pulpless teeth. *J Prosthet Dent.* 1992;68:421–27.
49. Ammar HH, Ngan P, Crout RJ, Mucino VH, Mukdadi OM. Three-dimensional modeling and finite element analysis in treatment planning for orthodontic tooth movement. *Am J Orthod Dentofac Orthop.* 2011;139:e59–71.
50. Roda-Casanova V, Pérez-González A, Zubizarreta-Macho A, Faus-Matoses V. Influence of Cross-Section and pitch on the mechanical response of NiTi endodontic files under bending and torsional Conditions-A finite element analysis. *J Clin Med.* 2022;11:2642.
51. Anitua E, Truchuelo Díez P, Pesquera Velasco J, Larrazabal N, Armentia M, Seco-Calvo J. Mechanical behavior of dental restorations: A finite element pilot study of Implant-Supported vs. Multiunit-Supported restorations. *Prosthesis.* 2024;6:413–28.
52. Demircan B, Demir P. 3D finite element analysis of stress distribution as a result of oblique and horizontal forces after regenerative endodontic treatment part II: comparison of material thickness. *BMC Oral Health.* 2023;23:869.

Publisher's note

Springer Nature remains neutral with regard to jurisdictional claims in published maps and institutional affiliations.